Astron. Astrophys. 318, 495–505 (1997)

ASTRONOMY AND ASTROPHYSICS

COYOTES IV: the rotational periods of low-mass Post-T Tauri stars in Taurus⋆

J. Bouvier[1,2], R. Wichmann[3], K. Grankin[4], S. Allain[1], E. Covino[5], M. Fernández[6,7], E.L. Martín[8], L. Terranegra[5], S. Catalano[9], and E. Marilli[9]

[1] Laboratoire d'Astrophysique, Observatoire de Grenoble, Université Joseph Fourier, B.P. 53X, F-38041 Grenoble Cedex, France (bouvier@gag.observ-gr.fr)
[2] Canada-France-Hawaii Telescope Corporation, P.O. Box 1597, Kamuela, HI 96743, USA
[3] Landessternwarte Königstuhl, D-69117 Heidelberg, Germany
[4] Astronomical Institute, Tashkent, 700052 Uzbekistan, CIS
[5] Osservatorio Astronomico di Capodimonte, Via Moiariello 16, I-80131 Napoli, Italy
[6] Max-Planck-Institut für Astronomie, Königstuhl, D-69117 Heidelberg, Germany
[7] Instituto de Astronomía, UNAM, Apdo. 70-264, 04510 México, D.F., México
[8] Instituto de Astrofísica de Canarias, E-38200 La Laguna, Tenerife, Spain
[9] Osservatorio Astrofisico di Catania, Citta' Universitaria, I-95125 Catania, Italy

Received 29 April 1996 / Accepted 1 July 1996

Abstract. We monitored the light variations of 58 weak-line T Tauri stars in Taurus, recently discovered in the X-ray wavelength range during the ROSAT All-Sky Survey. We derive photometric periods for 18 stars, all but one being ascribed to rotational modulation by stellar spots. The exception is a 37.6d period assigned to the orbital motion of a new pre-main sequence spectroscopic binary. Two thirds of the stars in our sample have an age larger than 10 Myr and up to 40 Myr, thus filling the observational gap that previously existed between T Tauri stars on convective tracks and ZAMS dwarfs for the determination of the rotational evolution of young low-mass stars. The rotational periods are found to range from 0.5 to 7.5 days, most periods being shorter than 5 days. This result provides direct evidence for the spin up of solar type stars as they contract on pre-main sequence radiative tracks, as predicted by recent models of angular momentum evolution. The paucity of long periods (P$\geq$5d, i.e., $V_{eq} \leq$10 km s^{-1}) in the sample of post-T Tauri stars leaves, however, the origin of the numerous slow rotators observed in young clusters an open issue.

Key words: stars: pre-main sequence – stars: rotation

1. Introduction

Measurements of the rotation rates of low-mass stars at different evolutionary stages are needed to constrain the various classes of models describing the angular momentum evolution of solar-type stars which have been proposed in the last few years. Starting with the earliest observable stars, i.e., pre-main sequence (PMS) T Tauri stars descending their Hayashi tracks, through young ZAMS dwarfs belonging to young clusters and older main sequence dwarfs, and up to the age of the Sun, the hope is ultimately to trace observationally the evolution of the surface rotation rate of solar-type stars as a function of age with as narrow a time sampling as possible. Major efforts have been devoted toward this goal in the last years by several groups, which resulted in the determination of the distribution of rotation rates among T Tauri stars (e.g., Bouvier et al. 1993, Edwards et al. 1993, Choi & Herbst 1996), late-type dwarfs in several young open clusters (e.g., Stauffer et al. 1989, Soderblom et al. 1993a, Prosser et al. 1995, O'Dell et al. 1995, Allain et al. 1996a, 1996b, 1996c) and older clusters (e.g., Radick et al. 1987, Soderblom & Mayor 1993).

A major observational gap still exists, however, between the oldest T Tauri stars with an age of a few Myr and the youngest cluster dwarfs at an age of 50 Myr. According to the models, it is precisely during these few 10 Myr of pre-main sequence evolution that the most rapid and the most drastic changes occur in the surface rotation rates of low-mass stars. In addition, the internal structure of low-mass stars rapidly evolves during this period, from a completely convective interior to a mostly radiative one, so that this phase is also the most suitable to study how structural changes impact onto the surface rotation rate.

Send offprint requests to: J. Bouvier

⋆ Based on observations made at the Mount Maidanak Observatory, Uzbekistan; at the Observatoire de Haute-Provence (CNRS), France; at the Observatorio Astronómico Nacional at San Pedro Mártir, Baja California, México; at the IAC80 telescope of Teide Observatory, Spain; at the Serra La Nave Observatory, Catania, Italy.

The 4th COYOTES campaign –Coordinated Observations of Young ObjecTs from Earthbound Sites– was specifically aimed at filling this gap by measuring the rotational period of post-T Tauri stars, i.e., low-mass T Tauri stars approaching the ZAMS on radiative tracks. An opportunity to do so was provided by the discovery of a number of such stars from ROSAT observations of star forming regions in the X-ray range. A large number of X-ray sources were detected, most of which turned out to be PMS stars based on their spectral properties (Neuhäuser et al. 1995, Alcala et al. 1995, Wichmann et al. 1996). We therefore selected a sample of X-ray sources identified as PMS stars from the study of Wichmann et al. (1996) in the Taurus cloud with the aim to measure their rotational periods. Although the exact evolutionary status of these stars was not known at the time, except that they were PMS stars, we show below using the photometry reported here that most of them appear to be *bona fide* post-T Tauri stars.

We briefly describe the organisation of the campaign and the multi-site observations in Sect. 2. The rotational periods and photometric properties of the sample stars are presented in Sect. 3. We show in Sect. 4 that most stars in the sample are T Tauri stars approaching the ZAMS on their radiative tracks and discuss the distribution of their rotational periods as well as its implications for the evolution of angular momentum in PMS solar type stars.

2. Observations

We observed two stellar samples containing respectively 25 and 26 ROSAT X-ray sources, spread over the whole Taurus star forming region, and identified as WTTS by Wichmann et al. (1996). One sample was monitored in the B- and V-band using diaphragm photometry. The other sample was observed using CCD photometry in the V-band. Unfortunately, the CCD runs were severely affected by poor weather and the data suffer from high sky background due to the proximity of the bright moon. A short description of data acquisition and reduction at the various sites is given below.

Diaphragm photometry was performed at the Mt. Maidanak Observatory, Uzbekistan, during two runs from November 2 to December 11, 1994 and from November 23, 1995 to January 13, 1996, respectively. Both runs were at the 0.48m telescope equipped with a pulse counting FEU-79 photomultiplier tube and a set of standard BV Johnson filters. A diaphragm of 28" was used and typical exposure times ranged from 20 up to 120 seconds, depending on the filter and on the object's brightness. The atmospheric extinction coefficients and the transformation to the standard system were derived from the observations of some 7 standard stars several times each night. The photometric reduction was performed using the standard procedures developed by Nikonov (1976).

Additional BV photoelectric observations were collected at the 84cm telescope of Observatorio Astronómico Nacional of San Pedro Mártir (B.C., México) from December 1 to 13, 1994. The telescope was equipped with the Lowell I photometer which consists of a P07029 photomultiplier and a set of Johnson Kron-Cousins $UBV(RI)_{KC}$ filters (Echevarria et al. 1991). About 15 BV standard stars from the list of Landolt (1983) were observed each night to transform the instrumental system in the standard BV system. A 20 arcsec diaphragm was used during the observations of standard and program stars. The data were reduced following the standard procedures and the mean extinction coefficients given by Schuster (1982) were adopted for the atmospheric extinction correction. The final observing errors, estimated from the observations of the standard stars are: $\sigma_B = 0.04, \sigma_V = 0.03$.

Diaphragm photometry has also been performed at Serra La Nave Observatory, Catania, Italy, over two observing periods in 1994 (November 22 to December 4) and 1995 (January 5, 6, 28, and 29), respectively, using the 91cm telescope equipped with a 9789QA PM tube. Measurements were obtained in two filters (B and V) with a diaphragm of 22 arcsec. Integration times of 5 and 10 sec per cycle were used for B and V, respectively, each measurement consisting of 3 cycles of integrations. For the determination of the night extinction and colour transformation coefficients to the Johnson standard system, some 10 standard stars from Landolt (1983) were observed nightly. Average atmospheric extinction coefficients for the observing run were adopted only in a few cases, when not enough standard stars could be measured. The reduction of the observations was performed using the PHOTOMETRY package written by C. Lo Presti available at Catania Observatory.

CCD observations were obtained from October 10 to 27, 1994, using the 0.82 m IAC80 telescope of Teide Observatory in the island of Tenerife, Spain. A CCD Thomson 1024x1024 with a pixel size of 0.43 arcsec was used. The exposure times with a V filter ranged from 60 to 300 s.

CCD photometry was also conducted at the 1.2m telescope of Observatoire de Haute-Provence, France, from February 4 to 14, 1995. A CCD Tek 512x512 with a pixel size of 0.76 arcsec was used to obtain images in the Johnson V and B filters. During one of the photometric nights of the run, secondary standards were observed in order to derive the mean B and V magnitude of the target stars.

Additional B&V CCD photometry was carried out from February 1 to 16, 1995, at the 1.5m telescope of the Observatorio Astronómico Nacional of San Pedro Mártir (B.C., México). A 1k Thompson CCD with a pixel size 0.20 arcsec was used. Integration times varied between 120 and 600s for the B band, and between 100 and 450s for the V band.

The photometric reduction of the CCD images was performed at CFHT using the NOAO/IRAF package DAOPHOT. The target star and several candidate comparison stars in the same image were measured. Proper comparison stars were identified by excluding those which exhibited intrinsic variations and usually only one star was selected, close to the object and of comparable brightness. The instrumental light curve of the comparison star was then subtracted from that of the target to obtain the differential light variations of the latter. The resulting overall error is of about 0.02 magnitude on average.

Table 1. Periods, photometric and stellar properties.

W	RXJ	P (d)	ΔV	ΔB	V	B	H_α (Å)	Sp.	T_{eff}	A_V	logL ($L_\odot$)	M ($M_\odot$)	Age (10^7yr)	R ($R_\odot$)	V_{eq} (km/s)
2	0403.4+1725	0.573	0.09	0.09	11.73	12.77	.0	K3	4775	0.1	-0.3	1.0	2.1	1.0	88
7	0406.8+2541	1.73	0.15		11.68	12.98	-6.2	K9	3960	0.	-0.1	0.5	0.1	1.9	56
9	0408.2+1956	3.02	0.26	0.31	13.08	14.27	-1.5	K2	4955	0.8	-0.6	0.9	$\geq$4.0	0.7	12
10	0409.2+2901	2.74:	0.04	0.05	10.59	11.43	1.7	K1	5105	0.	0.0	1.2	1.5	1.3	24
14	0412.8+2442	6.7	0.05	0.04	11.98	13.04	1.1	G9	5340	0.9	-0.2	0.9	3.9	0.9	7
18	0415.4+2044	1.83	0.08	0.09	10.66	11.37	2.6	K0	5236	0.	0.0	1.1	2.0	1.2	33
23	0420.4+3123	4.2	0.07		12.33	13.34	-.5	K4	4581	0.	-0.6	0.8	3.5	0.8	9
27	0423.7+1537	1.605	0.11	0.13	11.26	12.21	1.2	K2	4955	0.1	-0.2	1.0	1.9	1.1	35
28	0424.8+2643B	1.89	0.11		11.31	12.62	.9	K1	5105	1.4	0.3	1.5	0.6	1.8	48
32	0431.3+2150	2.71	0.11	0.14	10.84	11.68	1.9	K0	5236	0.1	-0.1	1.0	2.3	1.1	21
36	0432.7+1853	1.55	0.06	0.07	10.79	11.63	1.9	K1	5105	0.	-0.1	1.1	1.8	1.2	39
47	0438.7+1546	3.07	0.13	0.18	10.75	11.71	-.6	K1	5105	0.3	0.1	1.2	1.3	1.4	23
52	0444.4+2017	1.15	0.08	0.08	12.61	13.75	1.0	K1	5105	0.8	-0.4	0.8	$\geq$4.0	0.8	35
55	0445.8+1556	1.104	0.12	0.14	9.30	10.03	2.6	G5	5660	0.2	0.6	1.6	0.9	2.0	92
71	0457.0+1517	3.33	0.05	0.08	10.29	10.94	3.3	G3	5730	0.	0.1	1.1	2.7	1.1	17
72	0457.1+3142	$\geq$37.6	0.21	0.22	10.72	12.34	-.2	K2	4955	SB2					
73	0457.2+1524	2.39	0.09	0.10	10.30	11.25	1.7	K1	5105	0.2	0.2	1.4	0.8	1.7	36
75	0458.7+2046	7.53	0.06	0.07	11.91	13.15	.9	K7	4000	0.	-0.2	0.5	0.2	1.6	11

3. Results

Periods were searched for in the V-band and, when available, in the B-band light curves using 3 different methods: the periodogram analysis (Scargle 1982), the CLEAN deconvolution algorithm (Roberts & Dreher 1986) and the string-length estimator (Dworetsky 1983). False-alarm probabilities for the periodogram analysis (Horne and Baliunas 1986) were computed using a Monte-Carlo method as described in Bouvier et al. (1993; henceforth COYOTES I).

The results are listed in Table 1 and illustrated in Fig. 1. The star numbers are from Wichmann et al.'s (1996) Table 4. Photometric periods are detected in 18 stars among the 58 observed. Except for W10, all periods are detected at the 99.9% confidence level in the periodogram and confirmed by the results of the CLEAN and string-length analyses. W10's period is not detected in the raw periodogram analysis but is revealed by both the CLEANed periodogram and the string-length method.

The V-band light curves folded in phase are shown in Fig. 1 for 17 stars whose photometric periods are assumed to measure the stellar rotational periods (the remaining star, W72 with a period of at least 37.6d, is a double-line spectroscopic binary, see below). Most light curves are symmetric around minimum light, i.e., maximum spot visibility, which suggests that the modulation is driven by a single large spot group located at relatively high stellar latitudes. Note, however, the peculiar light curve of W9, which exhibits a deep and narrow minimum, somewhat reminiscent of eclipsing binary systems. Further support to this interpretation comes from the large amplitude of variability (ΔV=0.26mag), quite unexpected for a star of this age ($\geq$ 40 Myr). Other stars exhibit amplitudes ranging from 0.04 to 0.15 mag, and periods from 0.5d to 7.5d. The range of rotational periods exhibited by the present sample is discussed in Sect. 4.2.

The lower limit of 37.6 days set on the photometric period of the remaining star, W72, is quite remarkable. Such a long photometric period, if assumed to be the stellar rotational period, is quite unexpected for a WTTS. A perhaps related example is JW 648 with a period of 34.5d (Eaton et al. 1995) which, however, appears to be a classical T Tauri star based on its strong infrared excess. In contrast to spot-driven variability, no (B-V) color changes are observed along the photometric cycle of W72 (see Fig. 2). And a high-resolution spectrum obtained at OHP with the ELODIE spectrograph shortly after the COYOTES campaign reveals that W72 is indeed a double-line spectroscopic binary. We therefore ascribe the $\geq$37.6d photometric period to orbital instead of rotational modulation, pending an accurate spectroscopic determination. This star is not considered further in the following discussion.

In addition to the photometric periods, Table 1 also lists the photometric amplitudes measured in the V-band and, when available, in the B-band by fitting a sine curve to the light curves. The amplitudes are consistently if only slightly larger in the B-band than in the V-band, as expected from rotational modulation by cool spots (Bouvier et al. 1995). V and B magnitudes averaged over the duration of the campaign are listed as well.

The H_α equivalent width and spectral type, originally listed by Wichmann et al. (1996), are repeated in Table 1 for the sake of completeness. Effective temperatures were derived from spectral types using the scale provided by Cohen & Kuhi (1979). The stellar luminosity was computed from the V magnitude listed in Table 1, by applying a bolometric correction relevant to the star's spectral type (Johnson 1966) and correcting from the extinction on the line of sight that we derived from the B-V color

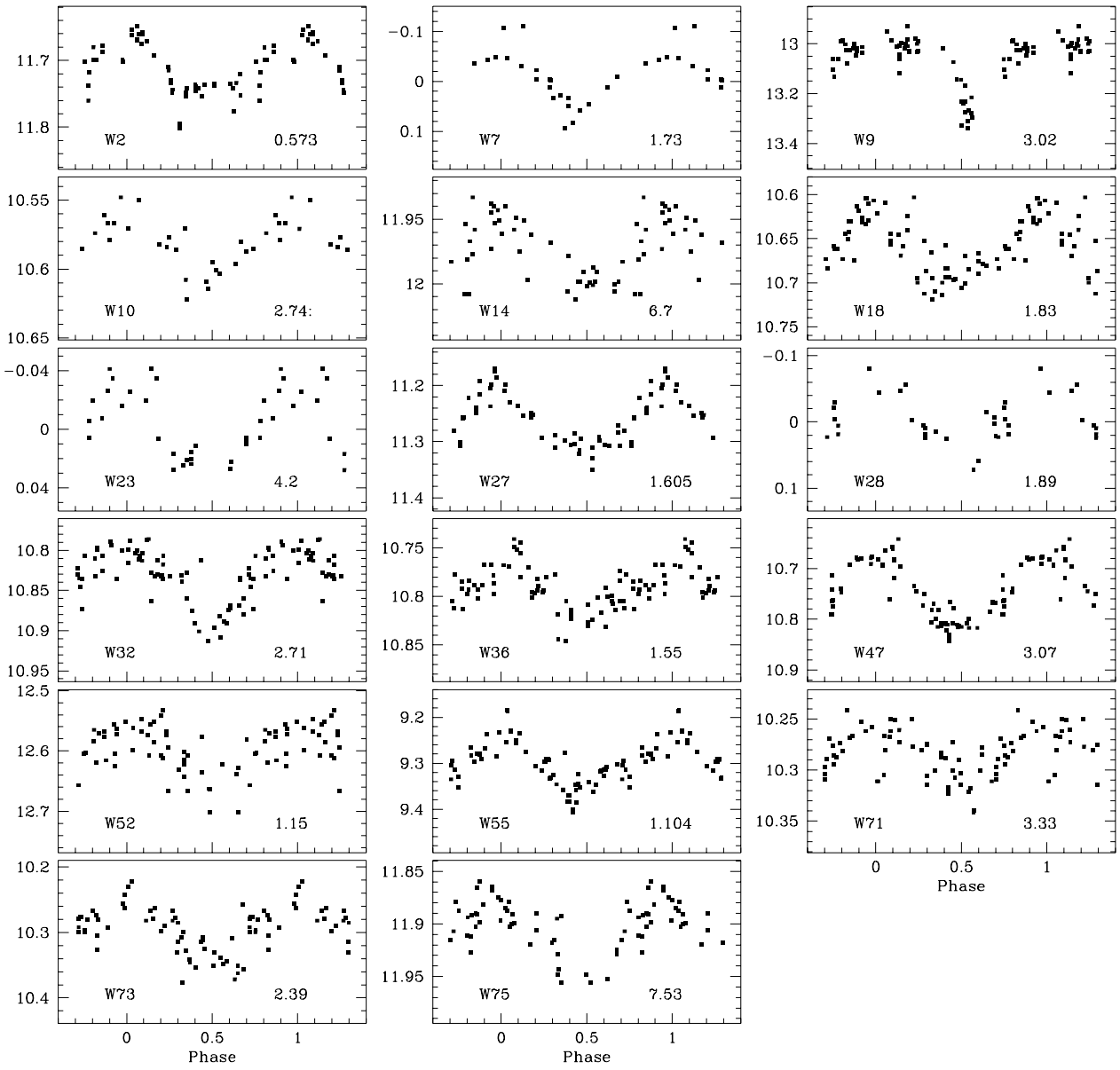

Fig. 1. V-band light curves folded in phase for stars with periodic light curves. The number of the star (as listed in Table 4 of Wichmann et al. (1996)) is given in the lower left corner of each panel and the value of the period (days) in the lower right corner. Zero-mean light curves are differential light curves obtained from CCD observations.

excess. The main source of error affecting the determination of the stellar luminosity lies in the assumption that all the stars are located at the average distance of the Taurus dark clouds, i.e., 140pc (Kenyon et al. 1994). The sample actually covers a projected area on the sky of approximately 15 by 15 degrees, corresponding to about 40 by 40 pc at this distance. Assuming the distribution of the stars is more or less uniform in all directions, some of them may thus be as close as 100pc and some other as far as 180pc. An error as large as 0.3 dex in logL may result.

Finally, we did not detect any periodicity in the light curves of the 40 other stars monitored during this campaign. Most of the non-detections pertain to stars whose light curves are affected by large temporal gaps: we found periods for only 3 (W7, W23, W28) of the 26 stars monitored during the CCD campaign, which was strongly affected by adverse weather. In contrast, periods were detected in 15 of the 32 well-sampled stellar light curves obtained from the diaphragm photometry campaign. We therefore believe that the failure to detect a period in the 23 stars observed during the CCD campaign primarily derives from the loose temporal sampling of their light curve. The remaining 17 stars observed with diaphragm photometry and for which we failed to detect a period have amplitudes of variability ranging from 0.03 and 0.07 mag. We cannot exclude that some of

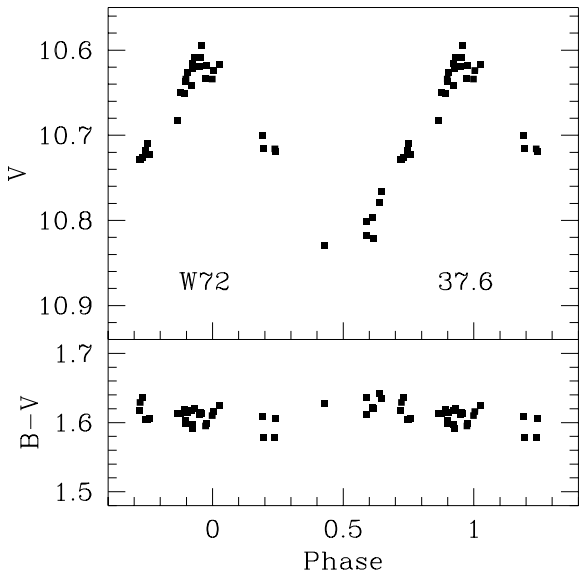

Fig. 2. V-band (upper panel) and B-V (lower panel) light curves of W72 folded in phase with a period of 37.6 days. The colorless variations, the shape and amplitude of the light curve suggests that the periodicity is due to the orbital motion of a binary system.

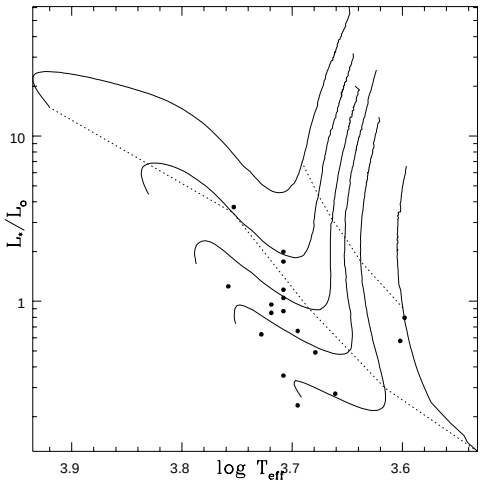

Fig. 3. HR diagram for the stars listed in Table 1. Solid curves are evolutionary tracks for stellar masses of 0.5, 0.8, 1.0, 1.2, 1.5, and 2.0$M_\odot$ (*from right to left*) which end at the ZAMS. The upper and lower dashed lines are isochrones for ages of 1 and 10 Myr, respectively (from Forestini's 1994 models).

them are long-period, low-amplitude variables. However, most of them exhibit variability in excess of the photometric error over a timescale of a few days. It is therefore most likely that the non-detection of a period in most of these 17 stars merely results from their low-level of modulation yielding low S/N light curves. We thus conclude that only few, if any, of the 40 stars for which we failed to detect a period are likely to be long-period variables.

4. Discussion

4.1. The stellar sample

The stellar sample was selected from the larger sample of 76 WTTS discovered by Wichmann et al. (1996) from both the ROSAT All-Sky-Survey (RASS) and pointed observations of the Taurus region. The spatial distribution of the new WTTS is shown in Fig. 3 of Wichmann et al.'s paper. As discussed there, the sources are more or less uniformely distributed over a wide region spanning 4h<R.A.(2000)<5h, 15°<Dec.(2000)<34°. Most of the stars are found located outside of the dense dark clouds in which optically-selected classical T Tauri stars usually cluster. On the basis of their widespread distribution, Wichmann et al. (1996) argued that the new WTTS have drifted away from the dark clouds and may therefore be older than previously known T Tauri stars.

The subsample of WTTS for which we report photometric periods share the same overall spatial distribution as the whole original sample. All 18 stars have spectral types between G3 and K9, and were identified as WTTS by Wichmann et al. (1996) on the basis of the strong lithium λ6707 line observed in their spectrum.

Using the stellar luminosity and the temperature listed in Table 1, we plotted the stars in the HR diagram (Fig. 3). PMS evolutionary tracks and isochrones from Forestini (1994) were used to derive the age and mass estimates listed in Table 1. For most stars, we derive ages that are significantly larger than those of previously known T Tauri stars. Because this result is central to the following discussion, we investigated how the mass and age estimates depend upon the choice of evolutionary tracks.

We therefore constructed new HR diagrams using evolutionary tracks and isochrones from D'Antona & Mazzitelli (1994) based either on the mixing-length theory of convection or on Canuto & Mazzitelli's (1992) convection model and deduced estimates of mass and age from these models. We find that the mass estimates are always in excellent agreement whichever set of evolutionary tracks is selected. The stellar ages derived from Forestini's isochrones and from the DM models based on MLT are also in very good agreement. However, age estimates based on the CM model of convection are systematically smaller by about 0.2 dex than those deduced from other models. While significant, this difference in age estimates does not modify the main conclusion that 2/3 of the stars in our sample have ages larger than 10 Myr and up to 40 Myr, while previously known optically-selected TTS in Taurus have ages of a few Myr at most (Gomez et al. 1992, Kenyon & Hartmann 1995).

Another source of uncertainty affecting the derivation of stellar parameters from the HRD is the effect of rotation upon stellar effective temperature. Martín & Claret (1996) showed that rotating PMS models are shifted towards lower effective temperature compared to non-rotating ones. The shift amounts to about 50K for a 0.8$M_\odot$ star rotating at 30 km s^{-1} at an age of 10 Myr. Because most of the stars discussed here lie on their radiative tracks, neglecting this effect does not substantially change the mass estimate (since the radiative tracks run

almost parallel to the T_{eff} axis) but underestimates stellar ages. As a result, the fastest rotators in our sample may be a few Myr older than the estimates listed in Table 1.

The relatively large ages thus derived for the stars studied here raises the issue of whether they actually belong to the Taurus association. Comparing the stellar properties and spatial distribution of the present sample with those of the sample of WTTS discovered by Walter et al. (1988) with the Einstein satellite, it appears most likely that the 2 samples are drawn from the same parental population of widespread young stars projected onto the Taurus star forming region. The similarity extends to the HR diagram, wherein stars of the 2 samples are found to span a mass range between $\leq$0.5 and 1.5$M_\odot$ and ages from a few Myr to 30 Myr or more. Hartmann et al. (1991) argued that the older stars located close to the ZAMS in Walter et al.'s sample, were actually low-mass members of the Cas-Tau B star group with an age between 30 and 50 Myr (see also the discussion in Walter & Boyd 1991). The same conclusion may well hold for the oldest stars in our sample, with an age of about 40 Myr according to their location in the HR diagram.

The sample studied here may thus include a population of low-mass stars that originated from different episodes of star formation in distinct regions of the Taurus-Auriga molecular complex. Some of these widespread WTTS might have escaped from the dark clouds, as suggested by Wichmann et al. (1996) and Sterzik & Durisen (1995), other might merely have formed in situ (Feigelson 1996). We discuss the possible implications of their diverse origin onto their rotational properties in Sect. 4.4. At any rate, those low-mass stars located on PMS radiative tracks with an age between 10 and 40 Myr appear to be *bona fide* post-T Tauri stars and this allows us to investigate the rotational properties of post-T Tauri stars as a new stellar group, which was one of the motivations for this study.

In summary, our stellar sample consists of 18 X-ray selected, low-mass young stars with an age ranging from a few Myr up to the ZAMS. Out of 17 stars whose rotational periods have been measured, 12 have an age larger than 10 Myr, and all but two are older than 4 Myr, the maximum age of T Tauri stars in the central dark clouds of Taurus. We therefore refer to these stars as post-T Tauri stars since their evolutionary status appears to be intermediate between that of optically-selected TTS on their convective tracks and ZAMS late-type dwarfs in young open clusters.

4.2. PMS evolution of rotation: observations

Rotational periods have now been measured for a few tens of weak-line T Tauri stars on convective tracks. Distributions of rotational periods for WTTS are shown in Bouvier et al. (1993) for Taurus stars and in Edwards et al. (1993) for Orion stars. In both cases, the distribution is relatively flat with WTTS spanning the range of rotational periods between 1.0 and 10 days. In order to compare the distribution of rotational periods between post-TTS and WTTS in Taurus, we selected from the compilation listed in Table 3 of Bouvier et al. (1995; henceforth COYOTES II) all WTTS with an age less than 10Myr and a mass less than 1.2$M_\odot$. This yields a sample of 14 young WTTS located on Hayashi convective tracks. We compare that sample with a sample of 12 post-T Tauri stars extracted from Table 1 above by selecting all stars with an age larger than 10 Myr and a mass less than 1.2$M_\odot$ (Fig. 4).

A 2-sided KS test applied on the cumulative distributions of the rotational periods of WTTS and post-TTS yields a probability of 0.02 that their are drawn from the same parental distribution. The histograms displayed in Fig. 4 show that PTTS tend to have shorter rotational periods than young WTTS. All but one post-TTS have periods shorter than 5 days while half of the WTTS have longer periods. If the distribution of periods of post-TTS was compared to that of CTTS instead of WTTS, the difference would be even larger since CTTS have longer periods than WTTS (see COYOTES I). This result thus provides direct evidence for the spin up of solar-type stars as they contract on PMS radiative tracks.

The observed difference between the distribution of rotational periods of WTTS and PTTS may be somewhat enhanced by the comparison of a sample of PTTS which mostly contains $\simeq$1$M_\odot$ stars with a sample of WTTS which mostly includes $\simeq$0.5$M_\odot$ stars. Bouvier (1991), after Vogel & Kuhi (1981), showed that the projected velocity of PMS stars increases with mass for masses larger than 1.2$M_\odot$. This 1.2$M_\odot$ limit, however, was estimated from PMS evolutionary models available at that time. Using modern evolutionary tracks, the mass limit decreases to around 1.0$M_\odot$. Hence, based on $v\sin i$ measurements, young PMS stars more massive than about 1$M_\odot$ appear to rotate faster on average than lower mass stars (see Strom 1994). There are unfortunately too few young 1$M_\odot$ WTTS with known rotational periods to build a statistically significant sample to which the sample of 1$M_\odot$ Post-TTS could be compared. Pending measurements of rotational periods for 1$M_\odot$ WTTS, it is therefore not straightforward to fully disentangle evolutionary effects from mass effects in the comparison of the rotational periods of the two above samples.

Similar histograms are drawn in Fig. 4 for equatorial velocities. Because they were computed using the stellar radius estimates listed in Table 1, values of equatorial velocities are not as accurate as those of rotational periods which are directly measured. A KS test yields a probability of 0.95 that the post-TTS and WTTS samples are similar. It thus appears that the equatorial velocity distributions of PTTS and WTTS bear a strong resemblance, even though their rotational period distributions greatly differ. This occurs because of the concomitant reduction of the stellar radius and rotational period as the star contracts on its radiative track, leading to smaller variations in the equatorial velocity, since $V_{eq} \propto R_\star/P$, than in the rotational period itself. A mild evolution of the equatorial velocity distribution with time could easily go unnoticed here, owing to the small size of the samples and because of the uncertainties associated with the derivation of equatorial velocities. From a spectroscopic study of PMS stars in the Orion nebula cluster, Duncan (1993) similarily concluded to the lack of a significant evolution of the $v\sin i$ distribution along radiative tracks.

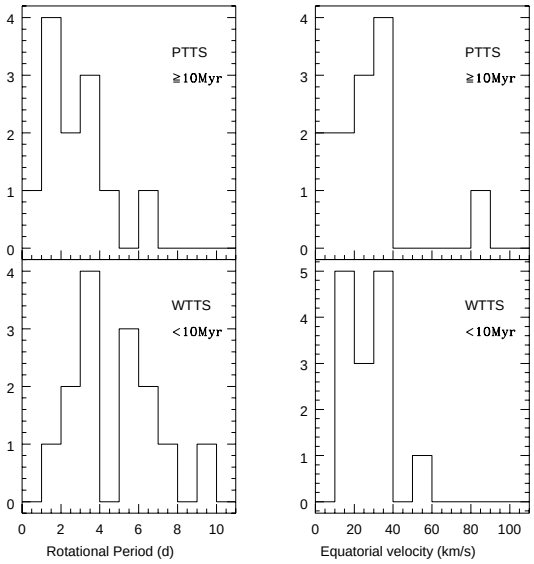

Fig. 4. Histograms of rotational periods (left) and equatorial velocities (right) for post-TTS (age$\geq 10^7$yr) of Table 1 (upper panels) and for WTTS (age$<10^7$yr) in the mass range 0.5-1.2$M_\odot$.

In spite of their statistical resemblance, it is apparent from Fig. 4 that the PTTS sample includes stars with both smaller ($\leq$10 km s^{-1}) and larger ($\geq$80 km s^{-1}) equatorial velocities than the WTTS sample. This trend, even though not statistically significant at this point, does go in the expected direction of a widening of the velocity distribution from the T Tauri phase to the ZAMS (Stauffer 1994, Bouvier 1994). That such a widening occurs has recently been clearly demonstrated from the measurements of projected velocities of a number of low-mass post-T Tauri stars in the Lupus and Chameleon star forming regions (Covino et al. 1996).

4.3. Comparison with models

The spin-up of solar-type stars on their PMS radiative tracks is expected to occur as a result of their decreasing moment of inertia. Once the PMS evolution is completed, the moment of inertia does not significantly change further, and magnetic winds brake the star down while evolving on the main sequence. So far, models were constrained by the measurements of the rotation of T Tauri stars on their convective tracks, young cluster dwarfs on or close to the ZAMS, and dwarfs belonging to both older clusters and the field. By providing rotational periods for post-T Tauri stars, the present study contributes to fill the observational gap that previously existed between young T Tauri stars and ZAMS dwarfs.

In order to constrain the models, rotational periods are preferable to projected velocities for at least two reasons. Firstly, periods are directly measured and are therefore more accurate than velocities, which are affected by projection effect and usually do not reach the required resolution to investigate the slowest rotators. Secondly, and perhaps more importantly, the rotational period, unlike the linear velocity, is directly related to the stellar *angular* velocity ($\Omega = 2\pi$/P) which is the prime physical parameter involved in the theoretical modelling of angular momentum evolution. The drawback is that derivation of rotational periods is much more time consuming than measurements of projected velocities, which explains why the latter are still much more numerous than the former.

Nevertheless, rotational periods have been lately derived for a rapidly increasing number of PMS stars on their convective tracks (e.g., Choi & Herbst 1996) as well as for a number of late-type dwarfs in young clusters (see O'Dell et al. 1995 and references therein, Allain et al. 1996a, 1996b). We have compiled data available for dwarfs and young TTS in the literature, combined them with the present results on post-TTS, and plotted the rotational periods as a function of time in Fig. 5. The following samples are drawn in order of increasing age: CTTS and WTTS of the Taurus cloud with a mass between 0.5 and 1.2$M_\odot$ selected from the compilation listed in COYOTES II; post-TTS in the same mass range selected from Table 1 above; Alpha Per G0-K0 dwarfs as well as Pleiades G0-K0 dwarfs selected from the compilation of O'Dell et al. (1995) and additional G0-K0 dwarfs of Alpha Per with the longest periods from the study of Allain et al. (1996b); and finally Hyades G0-K0 dwarfs from Radick et al. (1987).

We restricted the dwarf samples to spectral types between G0 and K0 and the TTS samples to masses between 0.5 and 1.2$M_\odot$, so that the observational data plotted in Fig. 5 can be considered as representative of the evolution of the rotational periods of stars around a solar mass. We stress, however, that the distribution of rotational periods for Alpha Persei dwarfs is probably not complete, and even much less so for Pleiades dwarfs, only a handful of which have known rotational periods in this mass range. In fact, the much more numerous measurements of the spectroscopic velocities of young cluster dwarfs indicate that a large fraction of them have $v\sin i$ less than 10 km s^{-1}, corresponding to P$\geq$5 days (Prosser 1992, Soderblom et al. 1993a, Allain et al. 1996c). This is not apparent in Fig. 5 because, with the exception of Allain et al.'s (1996b) study dedicated to slow rotators, previous determinations of rotational periods in the Alpha Persei and Pleiades clusters were severely biased towards rapid rotators. The issue of the very slow rotators in young clusters is further discussed in the next section.

The model shown in Fig. 5 is that of Bouvier (1994) as slightly modified by Bouvier & Forestini (1994, hereafter BF94). It describes the predicted evolution of the rotational period of a 1$M_\odot$ star from the T Tauri stage to the age of the Sun. The same model is illustrated in BF94 by plotting the linear velocity as a function of time, instead of the rotational period. Although the present study is only concerned with the rotation of PMS stars, we compare the model with data extending up to the age of the Sun because the rotational evolution of solar-type stars on the main sequence partly depends upon their PMS rotational history. Indeed, models are properly constrained only when taking into account observations spanning the whole age range from the youngest T Tauri stars to at least the age of the Sun.

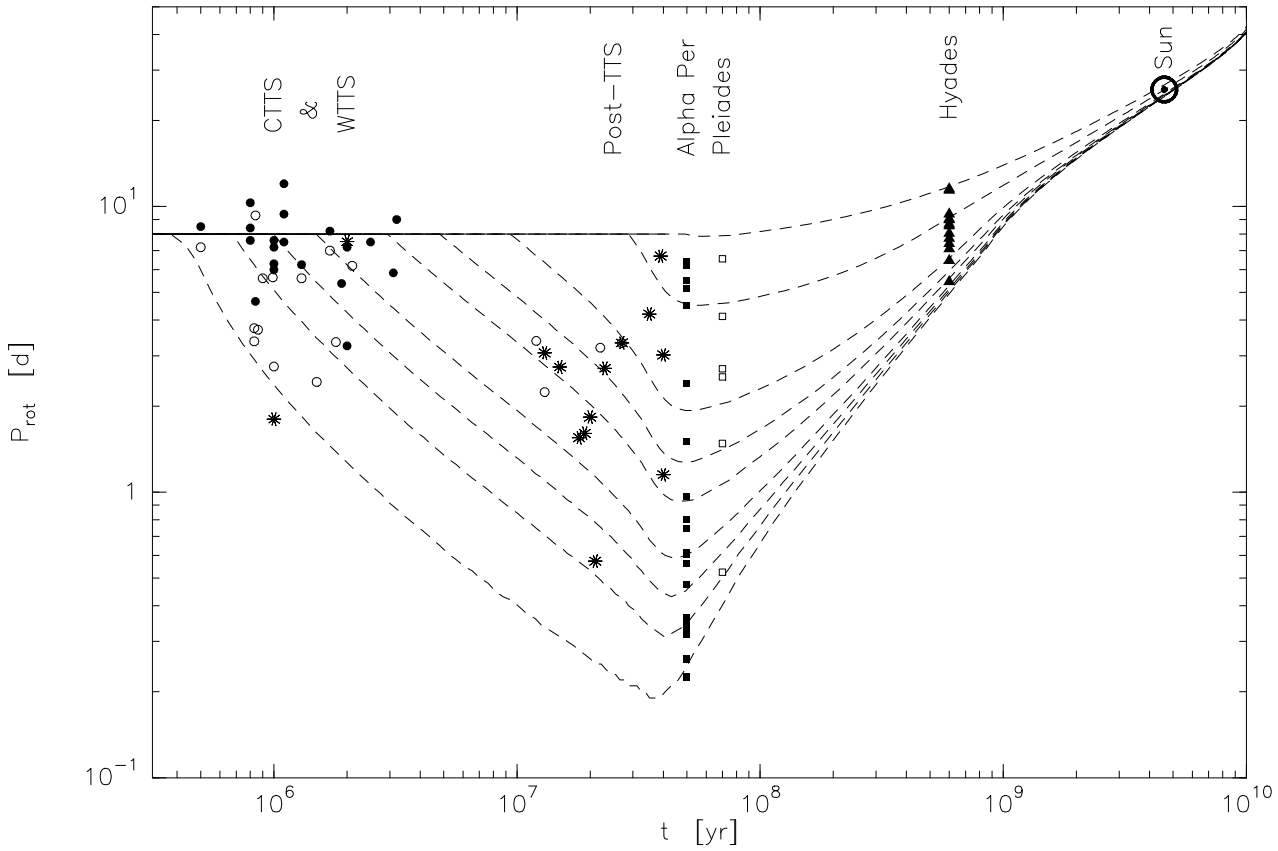

Fig. 5. The evolution of rotational periods with time for PMS stars in the 0.5-1.2$M_\odot$ range and G0-K0 dwarfs. The origin of all the data presented here is described in the text. CTTS are shown as filled circles, WTTS as open ones, and Post-T Tauri stars whose rotational periods are derived in this study are shown as starred symbols. Curves shows the predicted evolution of the rotational period of 1$M_\odot$ stars according to Bouvier & Forestini's (1994) model (see text for details).

The assumptions underlying the model are fully described in Bouvier (1994) and BF94 to which the reader is referred for details. In brief, it assumes solid-body rotation throughout the stellar interior, a Skumanich-type wind braking law ($dJ/dt \propto \Omega^3$) for slow rotators (≤ 8 km s^{-1}) and a milder ($dJ/dt \propto \Omega^2$) braking law for faster rotators. The dependence of the braking law upon angular velocity is continuous and quite similar in shape to the upper limit computed by Charbonneau (1992, Fig.1) for a linear dynamo while its amplitude is smaller at all rotation rates (see BF94). A detailed discussion of how such a model accounts for the observational data is beyond the scope of this paper and will appear elsewhere. We merely show here that it does predict an evolution of the dispersion of the rotational period distribution with time that agrees with current observational constraints.

It is now often assumed that T Tauri stars on their convective tracks are prevented from spinning-up as long as they remain magnetically coupled to their disk (see e.g. Königl 1991, Cameron & Campbell 1993, Shu et al. 1994 for models; Bouvier et al. 1993, Edwards et al. 1993 for observational support; Tout & Pringle 1992 for a different view). Each of the dashed curves shown in Fig. 5 starts at a different time of the PMS evolution of the star: the starting point corresponds to the age at which the magnetospheric star-disk coupling is assumed to cease, thus releasing the star which, from this point on, freely spins up as it contracts (the star does spin up in spite of wind braking, which carries some angular momentum away, though not enough to balance the effect of contraction during the PMS evolution). The time at which the star is released from the braking action of its disk is taken as a free parameter in this and other recent models (Keppens et al. 1995, Cameron et al. 1995). Finally, the choice of the initial rotational period of 8.0 days for stars coupled to their disk directly stems from the distribution of rotational periods derived in COYOTES I for CTTS which strongly peaks at that value.

The first rotational track displayed in Fig. 5 starts at an age of 4 10^5 yr. At that age, a 1$M_\odot$ star lies slightly below the birthline (Stahler 1988), in a region of the HRD where both CTTS and WTTS are actually observed (Kenyon & Hartmann 1995). By construction, this track provides a lower envelope to the distribution of rotational periods of young T Tauri stars that fits the observations. Following this track in time, the model then predicts an evolution of the lower envelope which complies well with observations of Post-TTS, of young and older cluster dwarfs and, eventually, of solar-type field stars. The observed spin up from the earliest T Tauri stars to Post-TTS within a timescale of 10 to 20 Myr is thus accounted for by the rapid

Table 2. Relative fraction of slow rotators in PTTS and young G dwarfs

Velocity (km s^{-1})	PTTS (10-40 Myr)	Alpha Per (50 Myr)	Pleiades (70 Myr)
$\leq$10	0.15	0.25	0.50
$\leq$20	0.30	0.50	0.80

reduction of the moment of inertia alone while only mild losses of angular momentum occur. Other recent models, whose assumptions differ from the one illustrated here (saturated instead of linear dynamo, core-envelope decoupling instead of uniform internal rotation), also predict spin-up for stars on their PMS radiative tracks (Soderblom et al. 1993b, Keppens et al. 1995, Cameron et al. 1995).

The starting points of the last 2 rotational tracks shown in Fig. 5 are set at an age of 30 and 50 Myr, respectively. Following the model of Königl (1991) and the numerical simulations by Cameron & Campbell (1993), these tracks illustrate how slow a star rotates upon its arrival on the ZAMS, should it remain coupled to its disk during a large fraction of its PMS evolution (BF94). Whether the accretion process in PMS stars can proceed for such a long time is, however, a matter of some debate. Recent surveys of IR excesses in T Tauri stars suggest that optically thick accretion disks survive more than 10 Myr around as much as 30% of the stars (Strom 1995). And Cameron et al. (1995) find that accretion rates as low as a few $10^{-11}M_{\odot}yr^{-1}$ are still sufficient to prevent the star from spinning-up. At such low accretion rates, the disk would become optically thin and therefore be more difficult to detect (Basri & Bertout 1989, Hartigan et al. 1990). Models which assume radiative core-convective envelope decoupling may allow for slightly shorter accretion timescales, though it is still a challenge for all models proposed so far to account for the slowest rotators ($V_{eq}\leq$10 km s^{-1}) observed in young clusters as we discuss below. And the paucity of long periods in the present sample of PTTS adds to the puzzle of the origin of these slow rotators.

4.4. Where are the slow rotators?

As noted above, the distributions of rotational periods illustrated in Fig. 5 for Alpha Per and Pleiades G dwarfs are incomplete and biased towards short periods. A more representative estimate of the actual distribution of rotation in these stars is provided by the much more numerous measurements of spectroscopic velocities. In particular, the extensive $v\sin i$ measurements performed by Soderblom et al. (1993a) and jointly by Allain et al. (1996c) and the CORAVEL group in Geneva allowed Allain et al. to statistically derive the complete distribution of *equatorial* velocities of Pleiades G dwarfs. It thus appears that by the age of the Pleiades (70 Myr) 50% of solar-type stars have equatorial velocities in the range from 5 to 10 km s^{-1} . In the slightly younger Alpha Persei cluster, this fraction is about 25% as judged from $v\sin i$ measurements (Stauffer et al. 1989, 1993, Prosser 1992).

The fraction of slow rotators amongst low-mass PTTS listed in Table 1, as well as amongst G dwarfs of the Alpha Per and Pleiades clusters is listed in Table 2 and suggests a smooth progression of the relative number of slow rotators between the age of Post-TTS and the Pleiades. The evolution from Alpha Per to Pleiades may be accounted for by magnetic braking acting on the outer convective envelope (Soderblom et al. 1993b, Fig.4). However, to increase the number of ultraslow rotators (USRs, i.e., with a velocity less than 10 km s^{-1}) between 10 and 50 Myr is much more difficult because it is precisely between 10 and 30 Myr that the moment of inertia of a solar-mass star decreases the fastest as the radiative core develops and the convective envelope recedes. Indeed, current models still fail to predict a significant fraction of stars with an equatorial velocity below 10 km s^{-1} at an age of 50 Myr.

One possible solution to the USR problem is to allow the magnetic interaction between the star and its disk to last long enough to prevent the star from spinning up during its approach to the main sequence (BF94). If this were correct, one would expect to find a significant fraction of USR among post-T Tauri stars. However, Table 2 shows that, with admittedly limited significance, within our PTTS sample the fraction of USR is much less than in young clusters.

The paucity of USRs among X-ray discovered PTTS might result from the relatively poor sensitivity of the RASS which is strongly biased towards the detection of the brightest X-ray sources (e.g., Wichmann et al. 1996). A correlation between X-ray flux and rotation has been reported for PMS stars on convective tracks (Bouvier 1990, Damiani & Micela 1995, Neuhäuser et al. 1995) and for late-type stars in young clusters (Stauffer et al. 1994). In particular, Stauffer et al. (1994) showed that the X-ray luminosity of late-type dwarfs in the Pleiades drops rapidly and by as much as one order of magnitude for stars with $v\sin i$ less than 10 km s^{-1} compared to faster rotators. It is yet unknown whether a similar relationship holds for PMS stars on radiative tracks and our sample is too small to address this issue. If such a relationship existed, the RASS X-ray selection would induce a bias towards the detection of fast rotators, thus possibly accounting for the lack of USRs in the PTTS sample. Unbiased detection of post-T Tauri stars in star forming regions via either proper motion surveys or deep X-ray studies is needed to settle this issue.

Alternatively, though probably less likely, the lack of USRs in the sample of PTTS could also bear direct relationship with the origin of these stars. Sterzik & Durisen (1995) argued that the population of WTTS discovered in the X-ray range and spread around dense molecular clouds may correspond to high tangential velocity stars ejected from the central clouds. They showed that few-body gravitational encounters occuring at the end of the protostellar collapse could produce escapers with velocities large enough to be located a few tens of parsecs away from their parental cloud within a few Myr.

Assuming that protostellar gravitational encounters are the origin of the PTTS studied here, one then expects the sample to be biased towards relatively fast rotators. This is because, as noted by Sterzik & Durisen (1995), close encounters would

probably strip the circumstellar material of the escaper, which would then become a WTTS early in its PMS evolution. As depicted in the previous section, such a star that gets rid of its circumstellar disk early in its evolution spins up and approaches the ZAMS as a moderate or fast rotator. This could conceivably explain why so few slow rotators are found among the PTTS sample.

As stated by Sterzik & Durisen (1995), however, it remains to be seen whether the large number of widespread WTTS dicovered by ROSAT around the Taurus molecular cores, as well as their mass function, can indeed be accounted for by such a mechanism. And whether this mechanism does apply to the present sample of PTTS awaits measurements of their radial and tangential velocities (see Feigelson 1996). The origin of USRs in open clusters thus remains an open issue.

5. Conclusion

Several models have been proposed in the last years to account for the observed evolution of the surface rotation rates of solar-type stars from their earliest T Tauri stage up to the age of the Sun. It is now widely believed that the extremely fast surface rotation rates observed for some ZAMS dwarfs result from structural changes occuring in the stellar interior, namely the reduction of the stellar moment of inertia, as PMS stars contract towards the main sequence. This interpretation is supported by the results reported here which provide direct evidence for enhanced angular velocity in PMS stars approaching the ZAMS on their radiative tracks.

The main challenge for theoretical models has now become to account for the existence of the large number of very slow rotators observed on the ZAMS. In this respect, the paucity of slow rotators in our sample of stars approaching the ZAMS is even more puzzling. We suggest that the progenitors of ZAMS slow rotators are themselves slow rotators on their PMS radiative tracks and that they might have consequently been missed by the ROSAT All-Sky-Survey which is only sensitive to the brightest X-ray sources. This could be the case in particular if the correlation found between X-ray flux and rotation rate for young T Tauri stars and open cluster dwarfs extends to PMS stars on their radiative tracks. In order to address this issue, unbiased samples of post-T Tauri stars have to be constructed via, e.g., large-scale, sensitive proper motion surveys of star forming regions.

Acknowledgements. MF would like to acknowledge the staff of the OAN at San Pedro Mártir for their help during the observations. This work was partially supported by the DGAPA-UNAM through project IN101794 and the spanish Ministerio de Educación y Ciencia. RW was supported by DFG under grant KR 1053/3. ELM thanks Maria Rosa Zapatero-Osorio for helping with the IAC80 observations. SC thanks Antonio Frasca for support to the observations and reduction of Catania data.

References

Alcala J.M., Krautter J., Schmitt J.H.M.M., Covino E., Wichmann R., Mundt R. 1995, A&AS 114, 109
Allain S., Bouvier J., Prosser C.F., Marschall L.A., Laaksonen B.D. 1996a , A&A 305, 498
Allain S., Fernandez M., Martin E., Bouvier J. 1996b, A&A in press (COYOTES III)
Allain S., Mayor M., Queloz D., Fernández M., Martín E.L., Bouvier J., Mermilliod J.C. 1996c, in: 9th Cambridge Workshop on Cool Stars, Stellar System and the Sun, eds R. Pallavicini & A.K. Dupree, in press
Basri G., Bertout C. 1989, ApJ 341, 345
Bouvier J. 1990, AJ 99, 946
Bouvier J. 1991, in: Angular Momentum Evolution of Young Stars. S. Catalano & J.R. Stauffer, eds, Kluwer Academic Publishers, Dordrecht,NATO ASI Series, p.41
Bouvier J. 1994, in: The 8th Cambridge Workshop Cool Stars, Stellar System and the Sun, ed. J.-P. Caillault, ASP Conf. Ser., Vol. 64, p. 151
Bouvier J, Forestini M. 1994, in "Circumstellar dust disk and planetary formation", 10th IAP meeting, eds Ferlet, p. 347 (BF 94)
Bouvier J., Cabrit S., Fernández M., Martín E.L., Matthews J. 1993, A&A 272, 167 (COYOTES I)
Bouvier J. Covino E., Kovo O., Martin E.L., Matthews J.M., Terranegra L., Beck S.C. 1995, A&A 299, 89 (COYOTES II)
Cameron A.C., Campbell C.G. 1993, A&A 274, 309
Cameron A.C., Campbell C.G., Quaintrell H., 1995, A&A 298 133
Canuto V.M., Mazzitelli I. 1992, ApJ 389, 724
Charbonneau P. 1992, in: 7th Cambridge Workshop on Cool Stars, Stellar Systems, and the Sun, ASP Conf. Ser., Vol.26, M.S. Giampapa & J.A. Bookbinder eds, p.417
Choi P.I., Herbst W. 1996, AJ 111, 283
Cohen M., Kuhi L.V. 1979, ApJS 41, 743
Covino E., et al. 1996, in: 9th Cambridge Workshop on Cool Stars, Stellar System and the Sun, eds R. Pallavicini & A.K. Dupree, in press
D'Antona F., Mazzitelli I 1994, ApJS 90, 467
Damiani F., Micela G. 1995, ApJ 446, 341
Duncan D.K. 1993, ApJ 406, 172
Dworetsky M.M. 1983, MNRAS 203, 917
Eaton N.L., Herbst W., Hillenbrand L.A. 1995, AJ 110, 1735
Echevarria J., Murillo J., Hiriart D. 1991, Manual de Usuario del Fotómetro Cuenta PulsosII, Observatorio Astronómico Nacional, Mexico
Edwards S. et al. 1993, AJ 106, 372
Feigelson E.D. 1996, ApJ, in press
Forestini M. 1994, A&A 285, 473
Gomez M. et al. 1992, AJ 104, 762
Hartigan P., Hartmann L., Kenyon S.J., Stron S.E., Skrutskie M.F. 1990, ApJ 354, L25
Hartmann L., Stauffer J.R., Kenyon S.J., Jones B.F. 1991, AJ 101, 1050
Horne J.H., Baliunas S.L. 1986, ApJ 302, 757
Johnson 1966, ARA&A 4, 197
Kenyon S.J., Dobrzycka D., Hartmann L. 1994, AJ 108, 1872
Kenyon S.J., Hartmann L. 1995, ApJS 101, 117
Keppens R., MacGregor K.B, Charbonneau P., 1995, A&A 294, 469
Königl A. 1991, ApJ 37, L39
Landolt A.U. 1983, AJ 88, 439
Martín E.L., Claret A. 1996, A&A 306, 408

Neuhäuser R., Sterzik, M.F., Schmitt J.H.M.M., Wichmann R., Krautter J. 1995, A&A 297, 391
Nikonov 1976, Izv. Krymsk. Astrofiz. Obs. 54, 3-23.
O'Dell M.A., Panagi P., Hendry M.A., Cameron A.C. 1995, A&A 294, 715
Prosser C.F. 1992, AJ 103, 488
Prosser C.F. et al. 1995, PASP 107, 211
Radick R.R., Thompson D.T., Lockwood G.W., Duncan D.K., Bagget W.E. 1987, ApJ 321, 459
Roberts D.H., Dreher J.W. 1986, AJ 93, 968
Scargle J.D. 1982, ApJ 263, 835
Schuster W.J. 1982, Rev. Mex. Astron. Astrof. 5, 149
Shu F., Najita J., Ostriker E., Wilkin F., Ruden S., Lizano S. 1994, ApJ 429, 781
Soderblom D.R., Mayor M. 1993, ApJ 402, L5
Soderblom D.R., Stauffer J.R., Hudon J.D., Jones B.F. 1993a, ApJS 85, 315
Soderblom D.R., Stauffer J.R., MacGregor K.B., Jones B.F. 1993b, ApJ 409, 624
Stahler S.W. 1988, ApJ 332, 804
Stauffer J.R. 1994, in: The 8th Cambridge Workshop Cool Stars, Stellar System and the Sun, ed. J.-P. Caillault, ASP Conf. Ser., Vol. 64, p. 163
Stauffer J.R., Hartmann L.W., Jones B.F. 1989, ApJ 346, 160
Stauffer J.R., Prosser C.F., Giampapa M.S., Soderblom D.R., Simon T. 1993, AJ 106, 228
Stauffer J.R., Caillault J.P., Gagne M., Prosser C.F., Hartmann L.W. 1994, ApJS 91, 625
Sterzik M.F., Durisen R.H. 1995, A&A 304, L9
Strom S.E. 1994, in: The 8th Cambridge Workshop Cool Stars, Stellar System and the Sun, ed. J.-P. Caillault, ASP Conf. Ser., Vol. 64, p. 211
Strom S.E. 1995, Rev. Mex. A&A Ser. Conf., Vol.1, p.317
Tout C.A., Pringle J.E. 1992, MNRAS 256, 269
Vogel S.N., Kuhi L.V. 1981, ApJ 245, 960
Walter F.M., Boyd W.T. 1991, ApJ 370, 318
Walter F.M., Brown A., Mathieu R.D., Myers P.C., Vrba F.J. 1988, AJ 96, 297
Wichmann R. et al. 1996, A&A, in press

This article was processed by the author using Springer-Verlag LaTeX A&A style file *L-AA* version 3.